Available online at www.sciencedirect.com
ScienceDirect
Journal of Volcanology and Geothermal Research 160 (2007) 249–262
Journal of volcanology and geothermal research
www.elsevier.com/locate/jvolgeores

An infrasound array study of Mount St. Helens

Robin S. Matoza [a,*], Michael A.H. Hedlin [a,1], Milton A. Garcés [b,2]

[a] *Laboratory for Atmospheric Acoustics (L2A), Institute of Geophysics and Planetary Physics, Scripps Institution of Oceanography, University of California, San Diego, USA*
[b] *Infrasound Laboratory (ISLA), University of Hawaii, Manoa, USA*

Received 21 February 2006; received in revised form 22 August 2006; accepted 3 October 2006
Available online 6 December 2006

Abstract

The ongoing activity of Mount St. Helens provides an opportunity to study the infrasonic wavefield produced by an active, silica-rich volcano. In late October 2004, as a pilot experiment for the Acoustic Surveillance for Hazardous Eruptions (ASHE) project, we deployed two infrasound arrays, each co-located with a broadband seismometer and weather station, to continuously record seismo-acoustic signals from Mount St. Helens. The nearest array, Coldwater, was deployed on the northern flank of the volcano, ~ 13 km from the summit. The second array, Sacajawea, was deployed ~ 250 km east of the volcano, at a distance where stratospherically ducted acoustic waves may be expected during the winter. This paper presents an overview of the experimental setup, and preliminary results from this unique data set. Eruptions on January 16th 2005 and March 9th 2005 produced strong infrasonic signals. The aseismic January 16th eruption signal lasted ~ 9.4 min beginning at ~ 11:20:44 01/16/05 UTC, while the March 9th eruption signal lasted ~ 52.8 min beginning at ~ 01:26:17 03/09/05 UTC, with the main steam and ash venting stage probably lasting ~ 7.2 min. The March 9th signal was an order of magnitude larger than the January 16th signal, and was clearly recorded 250 km east at the Sacajawea array. Infrasonic expressions of long period (LP) seismic events ('drumbeats') have also been intermittently observed, and are recorded as acoustic waves mimicking the waveform and temporal sequence of their seismic counterparts. These acoustic observations provide important constraints for source models of long period events and eruptions.
© 2006 Elsevier B.V. All rights reserved.

Keywords: volcano acoustics; infrasound; infrasound array; Mount St. Helens; long period event; eruption

1. Introduction

In this document, *infrasound* refers to acoustic energy traveling through the atmosphere at frequencies below the 20 Hz hearing threshold of the human ear. A large variety of natural and man-made phenomena produce infrasound, including avalanches, meteors, ocean waves, tornadoes, auroras, earthquakes, atmospheric nuclear tests, rockets, and supersonic aircraft (Bedard and Georges, 2000; Hedlin et al., 2002). The study of infrasound produced by volcanoes has a long history tracing back to 1883, when low frequency pressure signals from the eruption of Krakatoa were recorded on barometers distributed around the globe (Strachey, 1888). Almost a century later, infrasound radiated from the 1980 Mount St. Helens eruption was used to estimate the explosive yield of the main blast (e.g. Reed,

* Corresponding author. Mailing address: IGPP, SIO, Mail Drop 0225, U.C. San Diego, 9500 Gilman Drive, La Jolla, CA 92093-0225, USA. Tel.: +1 858 534 8119; fax: +1 858 534 6354.
E-mail address: rmatoza@ucsd.edu (R.S. Matoza).
[1] Mailing address: IGPP, SIO, Mail Drop 0225, U.C. San Diego, 9500 Gilman Drive, La Jolla, CA 92093-0225, USA.
[2] Mailing address: ISLA, 73-4460 Queen Kaahumanu Hwy., #119, Kailua-Kona, HI 96740-2638, USA.

0377-0273/$ - see front matter © 2006 Elsevier B.V. All rights reserved.
doi:10.1016/j.jvolgeores.2006.10.006

1987). The utility of dedicated infrasonic observations close to volcanoes has now been well established (e.g. Yamasato, 1997; Garcés and Hansen, 1998; Garcés et al., 1998, 1999; Hagerty et al., 2000; Ripepe and Marchetti, 2002; Johnson et al., 2003; Garcés et al., 2003; Johnson et al., 2004; Green and Neuberg, 2005; Johnson and Aster, 2005). However, to date, most volcano-infrasound studies have focused on small Strombolian-type explosions, simply because this type of activity is most abundant and reliable. Consequently, very little is known about the infrasound produced by large eruptions from silica-rich volcanoes. In addition, a large number of volcano-infrasound studies have acquired data using networks of low-cost microphones deployed near active vents (Johnson et al., 2003). Data acquired in this way are prone to wind noise and have a limited ability to discriminate volcanic sources of infrasound from other sources, although some progress has been made in this area (Johnson et al., 2006). Furthermore, microphones deployed close to vents are at risk of being destroyed during eruptions (Moran et al., in press), causing data loss at critical moments. The use of infrasound arrays as remote monitoring systems yields significant advantages in wind noise reduction and signal discrimination, as well as the ability to observe explosive eruptions at a safe distance.

The 2004–2006 eruption of Mount St. Helens (Dzurisin et al., 2005) has come at a time when the science of infrasound is modernizing rapidly. The 1996 Comprehensive Nuclear Test Ban Treaty (CTBT) has resulted in the ongoing deployment of a 60-station global network of infrasound arrays comprising part of the International Monitoring System (IMS) (Hedlin et al., 2002). After the third international workshop on volcanic ash and aviation safety in Toulouse (2003), the International Civil Aviation Organization (ICAO) requested that State Signatories of the Comprehensive Nuclear Test-Ban-Treaty (CTBT) investigate the use of the IMS for eruption warnings. In response, the Geological Survey of Canada (GSC), in collaboration with US infrasound experts in academia, developed the ASHE project as a proof of concept experiment to determine if timely eruption information could be provided to the Washington DC Volcanic Ash Advisory Center (VAAC). Mount St. Helens is currently an ideal active volcano with which to test the ASHE concept. Therefore, in late October 2004, the University of California, San Diego (UCSD), in collaboration with the GSC, began a pilot experiment consisting of two infrasound arrays recording seismo-acoustic signals from Mount St. Helens. This deployment has resulted in an excellent and unique volcano-acoustic data set.

Mount St. Helens is also one of the most closely monitored volcanoes in the world, observed by almost every geophysical and geological method. Consequently, the ongoing eruption of Mount St. Helens provides a unique opportunity to use state-of-the-art infrasound arrays to study pre-eruption and eruption signals produced by a silicic volcano, with the aim of integrating and cross-correlating these observations with existing seismic, geodetic, visual, and gas measurements. In this paper, we outline the experimental setup and present preliminary results from this infrasound data set. The research described in this paper was conducted with the support of the ASHE program, and adds to the growing body of literature on this subject, including work by researchers in Indonesia, Madagascar, France, Australia and the US who have studied the acoustics of volcanoes in the Indian Ocean and the Pacific for ash monitoring and basic research (Brown et al., 2005; Fee et al., 2005; Rambolamanana et al., 2005; Guilbert et al., 2005).

2. Data acquisition

In late October 2004, UCSD, in collaboration with the GSC, deployed two infrasound arrays to record signals from Mount St. Helens. The nearest array, Coldwater, was deployed on the northern flank of Mount St. Helens (Fig. 1), ~ 13 km from the summit. This array is located in a young forest owned by the Weyerhaeuser forest products company and provides a direct line-of-sight into the crater, as well as excellent low-noise recordings of acoustic signals from the volcano. The second array, Sacajawea, was deployed in Sacajawea State Park near Kennewick, WA, ~ 250 km east of the volcano (Fig. 1 inset). At this location, ray tracing for a typical winter atmosphere predicts that stratospherically ducted acoustic waves from Mount St. Helens would be recorded at the array. Each array consists of four MB2000 (DASE/Tekelec) broadband aneroid microbarometers arranged in a centered triangle with an aperture of ~ 100 m (Fig. 2). The array element locations are known to within 50 cm accuracy by differential GPS. Connected to each microbarometer are four ~ 15 m microporous hoses, which act as a spatial filter to preferentially sum coherent acoustic energy, and filter out spatially uncorrelated noise from wind turbulence (Hedlin et al., 2003). The central element is co-located with a Guralp CMG-40T broadband seismometer and Vaisala temperature, ultrasonic wind velocity, and wind direction sensors. The infrasound data sampled at 40 Hz have a flat response between 100 s and 17 Hz. The data are digitized using a 24-bit Nanometrics Polaris Trident digitizer and transmitted in real-time to a hub in Ottawa,

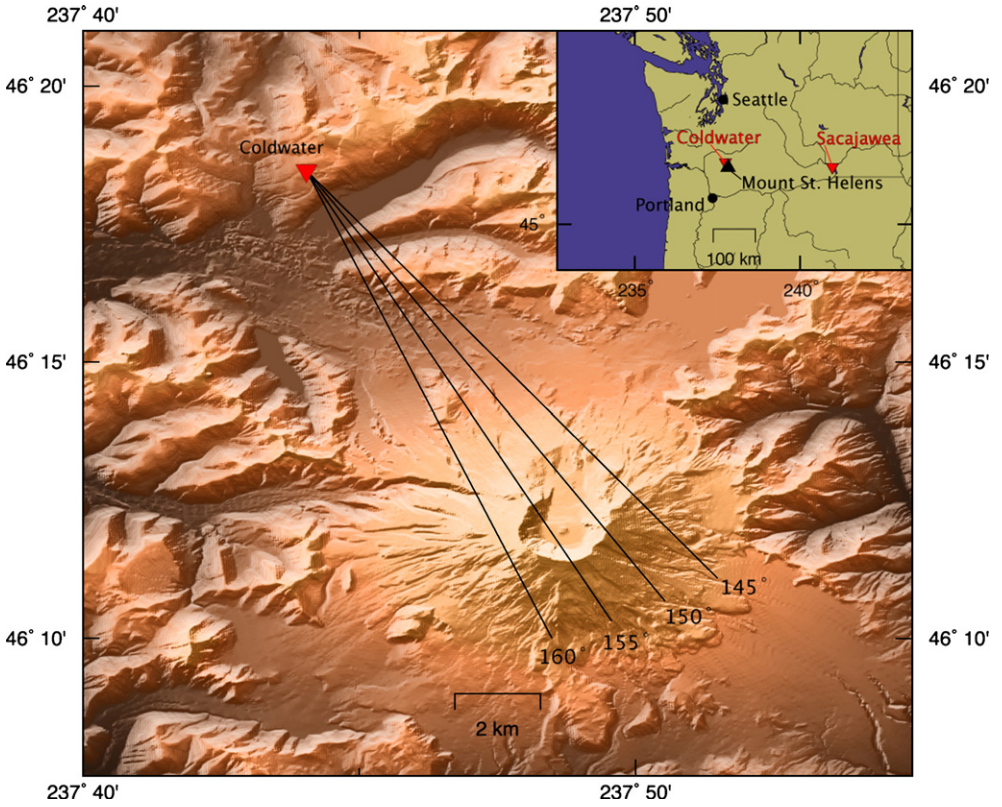

Fig. 1. Location of the Coldwater array (red triangle) with direct line-of-sight to Mount St. Helens ~ 13 km away. Black lines indicate the range of azimuths corresponding to Mount St. Helens as observed at Coldwater. Inset shows the location of both Coldwater and Sacajawea arrays in relation to Mount St. Helens and the northwestern US.

Canada and then to UCSD for archiving and analysis. Both arrays were withdrawn from the field on March 27th 2005 as the equipment was needed for another experiment. They were reinstalled on August 13th 2005, and continue to operate at the time of writing.

3. Advantages of infrasound arrays

Microbarometer arrays offer significant advantages over conventional networks of microphones. Primarily, arrays have the ability to discriminate signals on the basis of azimuth, and conventional or adaptive beam-forming techniques may then be applied to boost the signal to noise ratio of signals from a particular azimuth. Secondly, arrays yield the ability to estimate the phase velocity of signals, and therefore separate purely acoustic energy from mechanical shaking of the sensor by seismic energy. This ability to detect, discriminate, and enhance faint signals allows the array to be located at greater distance from the volcanic edifice. In turn, this enables more flexibility in site selection, so the array may be located in a wind-protected site such as a forest (Garcés et al., 2003). In contrast, sensors placed on top of a volcanic edifice are typically exposed to strong and variable winds, often obscuring the signals of interest. The microporous hoses attached to each array element also serve an essential role in suppressing wind noise, which exists at smaller spatial scales than coherent infrasound (Hedlin et al., 2003). This combination of spatial filters, wind-protected site selection, and array processing, is fully effective in separating coherent infrasound from incoherent wind noise.

4. Array processing with the progressive multichannel correlation method (PMCC)

The ambient infrasound field is rich and diverse, consisting of many forms of coherent and incoherent 'noise' that are simultaneously recorded with volcanic infrasound. We use the term *clutter* to describe coherent infrasound from sources other than the one of specific interest. To separate volcanic signals of interest from this background clutter, we use the progressive multichannel correlation method (PMCC). A detailed description of

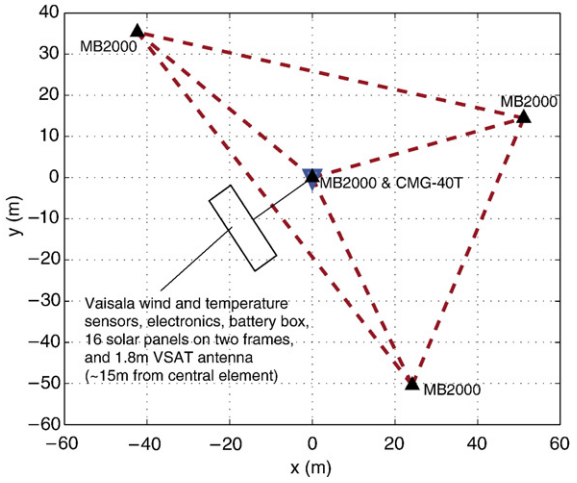

Fig. 2. Schematic of the Coldwater array geometry. Four MB2000 microbarometers (black triangles) are arranged in a centered triangle (depicted by red dashed lines). The central MB2000 is co-located with a Guralp CMG-40T broadband seismometer (blue triangle) and met station. Connected to each microbarometer are four ~ 15 m microporous hoses (not shown) acting as a spatial filter. The Sacajawea array has a similar layout.

the PMCC algorithm can be found in Cansi (1995), Cansi and Klinger (1997), and Garcés et al. (2003). PMCC uses correlation in the time domain to determine the time-delay Δt between different groupings of sensors i, j, k. Detections are assessed by seeking small values of r in the closure relation:

$$r_{ijk} = \Delta t_{ij} + \Delta t_{jk} + \Delta t_{ki}$$

A detection is registered if the consistency r is below a threshold value. This calculation is initially performed on a subset of three array elements, resulting in an initial azimuth and slowness estimate. Additional subsets of array elements are then progressively included in the calculation. If this results in a significant variation in the azimuth, velocity, or origin time estimate of a particular detection, the detection is discarded. The PMCC calculation is repeated for a series of time windows, at a designated number of frequency bands. The final result is a list of arrival times, azimuth of arrival, frequency content, speed, and amplitude of any coherent energy traveling across the array. PMCC provides an easy way to identify signals of interest from a very large amount of data. Once identified, we take a closer look at the waveforms using beamforming and other conventional signal processing techniques.

Array processing with the PMCC algorithm provides the ability to discriminate between signals from Mount St. Helens and clutter because each source of infrasound arrives with a unique azimuth, frequency content, amplitude, and speed. We primarily use arrival back azimuth to initially identify infrasound sources. For example, Fig. 3 shows a summary of PMCC detections at the Coldwater array between November 1st and 16th 2004 in the frequency band 1–5 Hz. The plot is typical of the data collected throughout the entire deployment. At all times we observe high frequency (3.5–5 Hz) cultural noise at ~ 200° (city of Portland) and ~ 240° (town of Kelso/Longview), and lower frequency (~ 1 Hz) signals from the Pacific Ocean (between 250° and 360°). The 2–3 Hz detections at ~ 153°, most notably between Julian days 313 and 318, turned out to be swarms of LP signals from Mount St. Helens (discussed below). The degree of scatter in the azimuth values for the separate sources is a complicated function of array response (array geometry), signal frequency content, signal to noise ratio, signal duration, wind conditions, source–receiver distance, and point source vs. distributed source effects, and is beyond the scope of this paper.

5. Results

5.1. Overview

The Coldwater and Sacajawea arrays were deployed at different distances to observe signals at close proximity and long range, respectively. The aim of this configuration was to demonstrate infrasonic monitoring at regional distances as part of the ASHE project. This paper presents results from the first deployment (October 30th 2004 to March 27th 2005). Data from the second deployment (August 13th 2005 to present) are not discussed in this paper. Observations at the Coldwater array have included: (1) infrasound associated with long period (LP) seismic events ('drumbeats'); (2) infrasound associated with well-documented eruptions on January 16th and March 9th 2005 and (3) infrasound occurring prior to the January 16th 2005 eruption, which may be linked to pre-eruptive processes.

The Coldwater array also recorded clutter in the form of low frequency noise from the direction of the Pacific Ocean, and high frequency cultural infrasound noise coming from the direction of the city of Portland, and other surrounding settlements (Fig. 3). Given the ~ 1 Hz frequency content of the Pacific detections, these signals are likely surf generated infrasound (Arrowsmith and Hedlin, 2005; Garcés et al., 2006). The signals from the urban areas (Portland and Kelso/Longview) could be generated by a number of sources, including airplanes during takeoff and landing at airports, power plants, traffic noise, or other industrial activity.

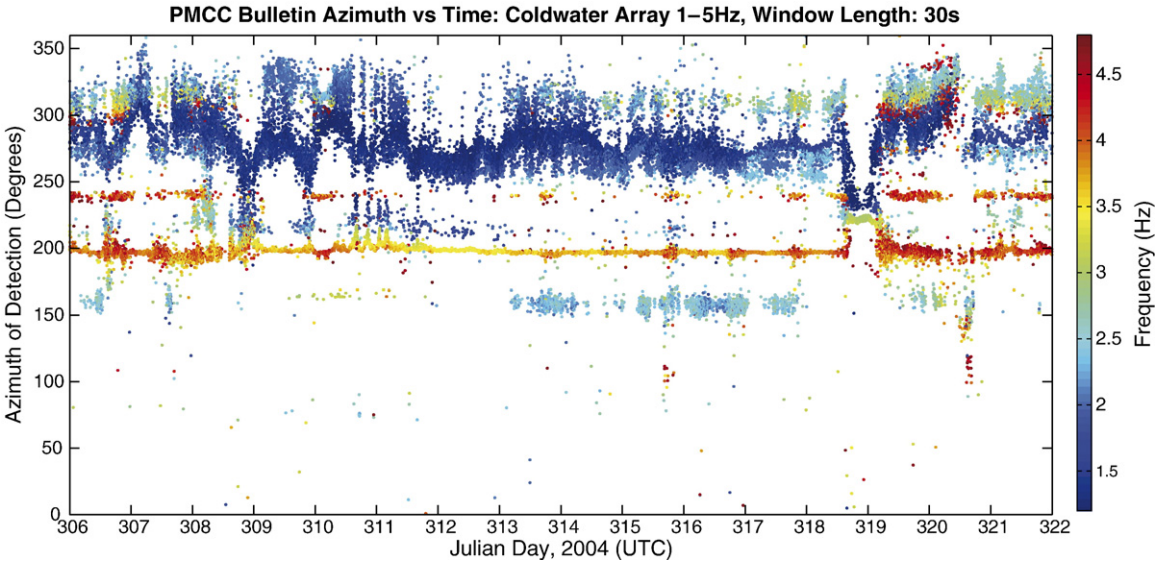

Fig. 3. Summary of PMCC detections at the Coldwater array, showing the arrival azimuth and frequency content (color) of coherent infrasound signals between Nov 1st and 16th, 2004 in the band 1–5 Hz. The continuous stream of high frequency (3.5–5 Hz — red dots) infrasound detections at ~ 200° and ~ 240° point directly at the nearby settlements of Portland (OR) and Kelso/Longview (WA). The lower frequency (1 Hz — dark blue dots) detections from a distributed source to the West (between 250° and 360°) point towards the Pacific Ocean. The bursts of 2–3 Hz detections at ~ 153° (especially between JD 313 and 318), turned out to be swarms of LP signals from Mount St. Helens. Plots like this give an overall picture of the characteristics of all of the separate infrasound sources recorded by the array at a given time, allowing one to identify signals of interest for detailed data analysis.

The Sacajawea array clearly recorded the March 9th 2005 eruption signal — the largest of signals produced by the volcano during the deployment (Figs. 8b and 9b). Sacajawea was subject to continuous infrasound from a nearby wind farm. This noise took the form of continuous droning propeller noise appearing at multiple discrete frequencies (Fig. 8b). This wind farm clutter was not loud enough to obscure the March 9th 2005 eruption signal, and was unambiguously detected using array processing.

5.2. Infrasonic long period events (drumbeats)

Seismicity during the 2004–2006 eruption of Mount St. Helens has been characterized by a sustained sequence of long period (LP) seismic events (0.5–5 Hz, Chouet, 1996) occurring beneath the dome. More specifically, the events are hybrid LP events (Lahr et al., 1994) owing to their broader band signal onset. These hybrid LP events have also been named seismic 'drumbeats' because of their highly repetitive and regular nature and constant delay time between successive events (Moran, 2005). Our observations show that these LP events have intermittent infrasonic *twins*. We define infrasonic *twins* as infrasonic arrivals with waveforms mimicking the seismic event waveforms and arriving after the seismic event with a velocity and time-delay appropriate for an acoustic wave. A clear example of this occurred in November 2004. Fig. 3 shows a summary of PMCC detections between November 1st and 16th 2004 in the frequency band 1–5 Hz. Bursts of 2–3 Hz detections coming from the direction of Mount St. Helens (~ 153° — see Fig. 1), occur between Julian days 313 and 318 (November 8th and November 13th 2004). To examine these detections more thoroughly, Fig. 4a shows 1 h of beamformed infrasound data from November 11th, 2004, compared with the co-located vertical seismic record. Both the infrasound and seismic data were filtered 2–4 Hz to isolate the LP signals. The infrasound beam is computed using a conventional time-delay beamformer (DeFatta et al., 1988), where the array gain in signal amplitude due to beamforming has been set to unity. The same beamformer is used throughout this article. Fig. 4b shows an expansion of 500 s of the record shown in Fig. 4a (indicated by box in Fig. 4a). In the lower box of Fig. 4b, the acoustic and seismic records have been amplitude-normalized, and the acoustic trace has been time-advanced by 38 s, the approximate time-delay for an acoustic wave following a seismic wave if both were simultaneously sourced at the volcano 13 km away. Once aligned in this manner, the infrasound signals mimic the seismic waveforms in

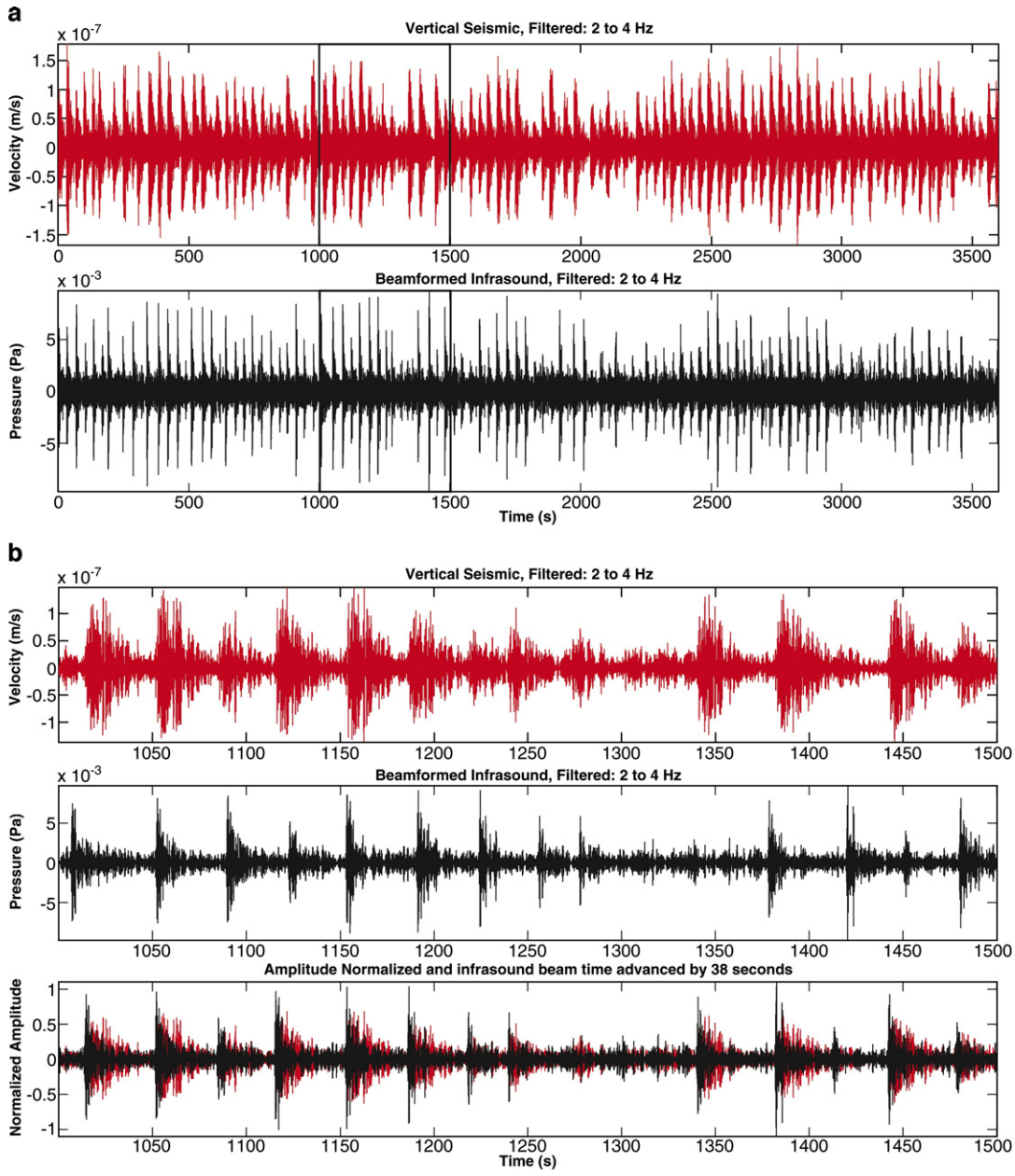

Fig. 4. (a) One hour of vertical seismic (top, red) and beamformed infrasound (bottom, black) recordings of LP events (drumbeats), on November 11th, 2004. Both series are filtered 2–4 Hz. The similarity of the two records is striking. Box indicates the time range covered in (b). (b) 500 seconds of vertical seismic (top, red) and beamformed infrasound (middle, black) LP events from the time indicated in (a). In the bottom panel, both signals have been amplitude-normalized, and the infrasound beam (black) has been time advanced by 38 s (predicted time-delay for the 13 km distance) and overlain with the co-located vertical seismic data (red). The infrasound waveforms mimic the seismic waveforms in amplitude and relative arrival time — indicative of a common source mechanism.

amplitude, sequencing, and duration. However, the characteristic long period coda observed in the seismic waves is less prominent in the infrasonic records. PMCC results and beamforming at a range of velocities show that the signals are propagating at acoustic velocities and are not caused by vibration of the pressure sensor by passing seismic waves. The amplitudes of the infrasonic LP events are typically $\sim 8\times10^{-3}$ pascals (Pa).

Not all seismic LP events have associated infrasonic twins. In November 2004 (Fig. 3), the infrasound twins were observed for 5 days between November 8th and November 12th. For the following 2 days they were

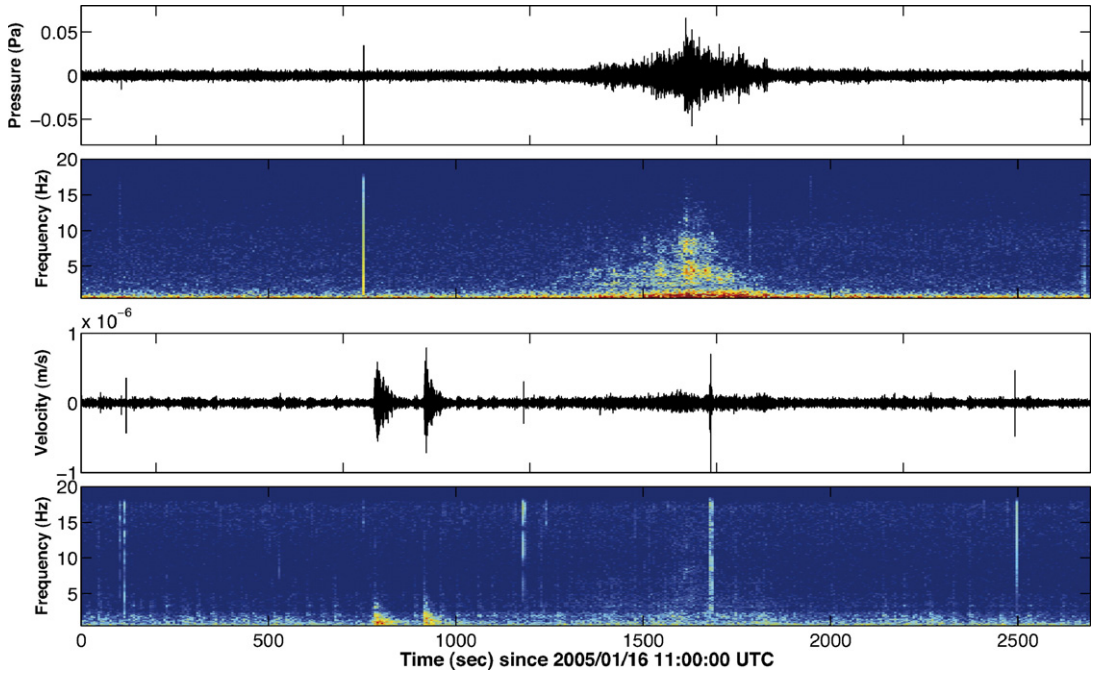

Fig. 5. Infrasound beam and its corresponding spectrogram (upper two panels), compared to the co-located vertical seismic channel and corresponding spectrogram (lower two panels) for the January 16th, 2005 eruption observed at Coldwater. The time series data are shown filtered 1–10 Hz. The eruption is distinguished by a clear infrasonic signal between ~ 1300 s and ~ 1800 s. The eruption is preceded ~ 500 s prior by two seismic LP events without infrasonic twins. No significant seismicity is associated with the eruption.

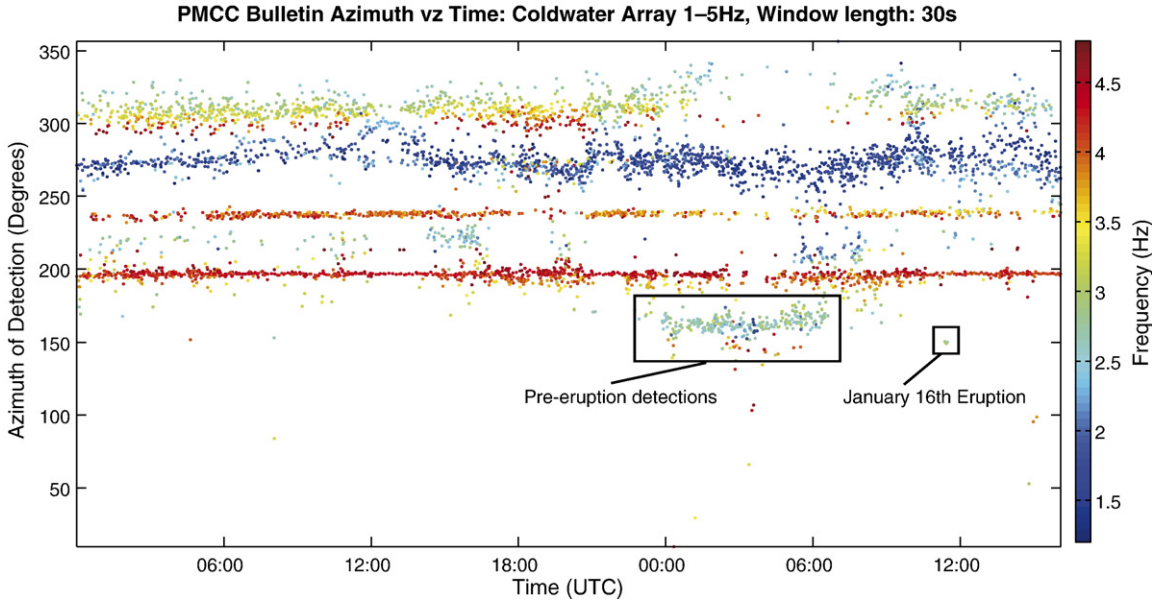

Fig. 6. Summary of PMCC detections spanning ~ 36 h prior to the eruption on January 16th 2005. Each coherent infrasound detection is plot at its arrival azimuth and color-scaled for its mean frequency. The main eruption is observed as a small cluster of blue (~ 2–3 Hz) dots at the appropriate time. Beginning at ~ 00:00 01/16/05 UTC, a stream of coherent infrasound events are detected for ~ 7 h from the direction of Mount St. Helens (~ 160°).

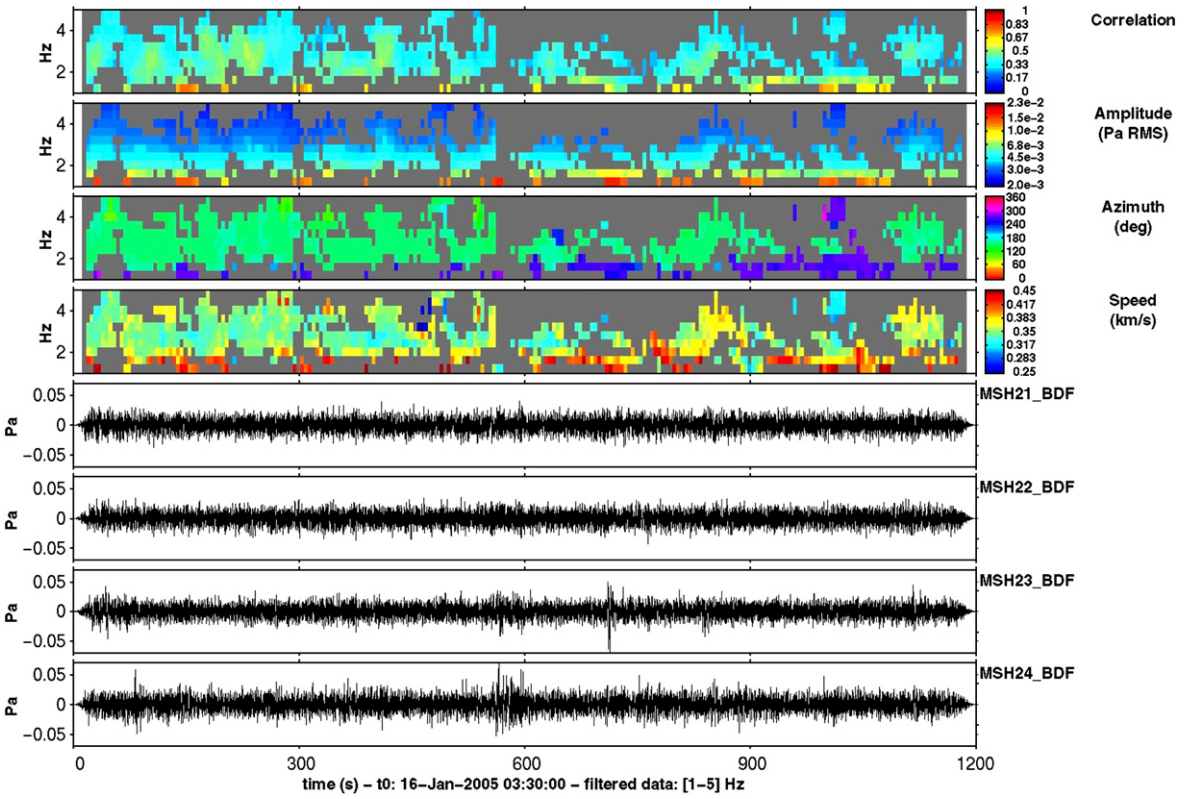

Fig. 7. PMCC analysis of a 20-minute selection of the pre-January 16th eruption infrasound detections depicted in Fig. 6. The top four panels show the frequency content of the signal vs. time, color-shaded according to the parameter labeled on the right-hand side. Correlation is that between different sensors of the array. Amplitude, azimuth, and speed describe how the signal propagated across the array. The lowermost four panels show the sensor time series data. The events have low signal to noise ratio and cannot be distinguished in the raw waveform data. However, PMCC clearly detects coherent energy at ~ 2–3 Hz coming from the direction of Mount St. Helens (~ 160° indicated by lime green in the azimuth panel).

absent, after which they reappeared for a further day on November 14th. The seismic channel was constantly recording LP events during this time.

5.3. Eruption infrasound

Two eruptions occurred during the November 2004–March 2005 deployment: on January 16th and March 9th 2005. The January 16th 2005 eruption occurred during the night, while the volcano was visually obscured by cloud cover. This eruption was effectively aseismic, so the only evidence that an eruption had occurred was loss of radio contact with USGS instruments deployed in the summit region, and visual evidence of ash deposits the following morning (http://vulcan.wr.usgs.gov). The March 9th 2005 eruption was a larger, dominantly phreatic (Moran et al., in press), explosive eruption that produced a plume of steam and ash in the atmosphere extending ~ 9 km above the dome. The infrasonic signals from both of these eruptions were recorded in full, with an excellent signal to noise ratio, on all four sensors of the Coldwater array (Figs. 5,8a,9a). The March 9th eruption was also clearly recorded on all four sensors of the Sacajawea array (Figs. 8b and 9b). In each case, PMCC processing yields a signal arriving directly from the direction of the summit area (Figs. 6 and 9).

5.3.1. January 16th 2005 eruption

Fig. 5 shows the beamformed infrasound data, compared with the co-located vertical seismic channel from the Coldwater array during the January 16th 2005 eruption. The data are shown filtered 1–10 Hz. The infrasound signal from the January 16th eruption, lasted ~ 9.4 min starting with an emergent onset at ~ 11:21:22 UTC and ending at ~ 11:30:47 UTC. Note that the travel time for infrasound from the volcano to the array is ~ 38 s, so the inferred eruption onset is ~ 11:20:44 UTC. The maximum amplitude of the infrasound signal at Coldwater was ~ 0.065 Pa.

The January 16th eruption was also preceded by ~ 7 h of coherent infrasound detections coming from the direction of Mount St. Helens. Fig. 6 shows a summary

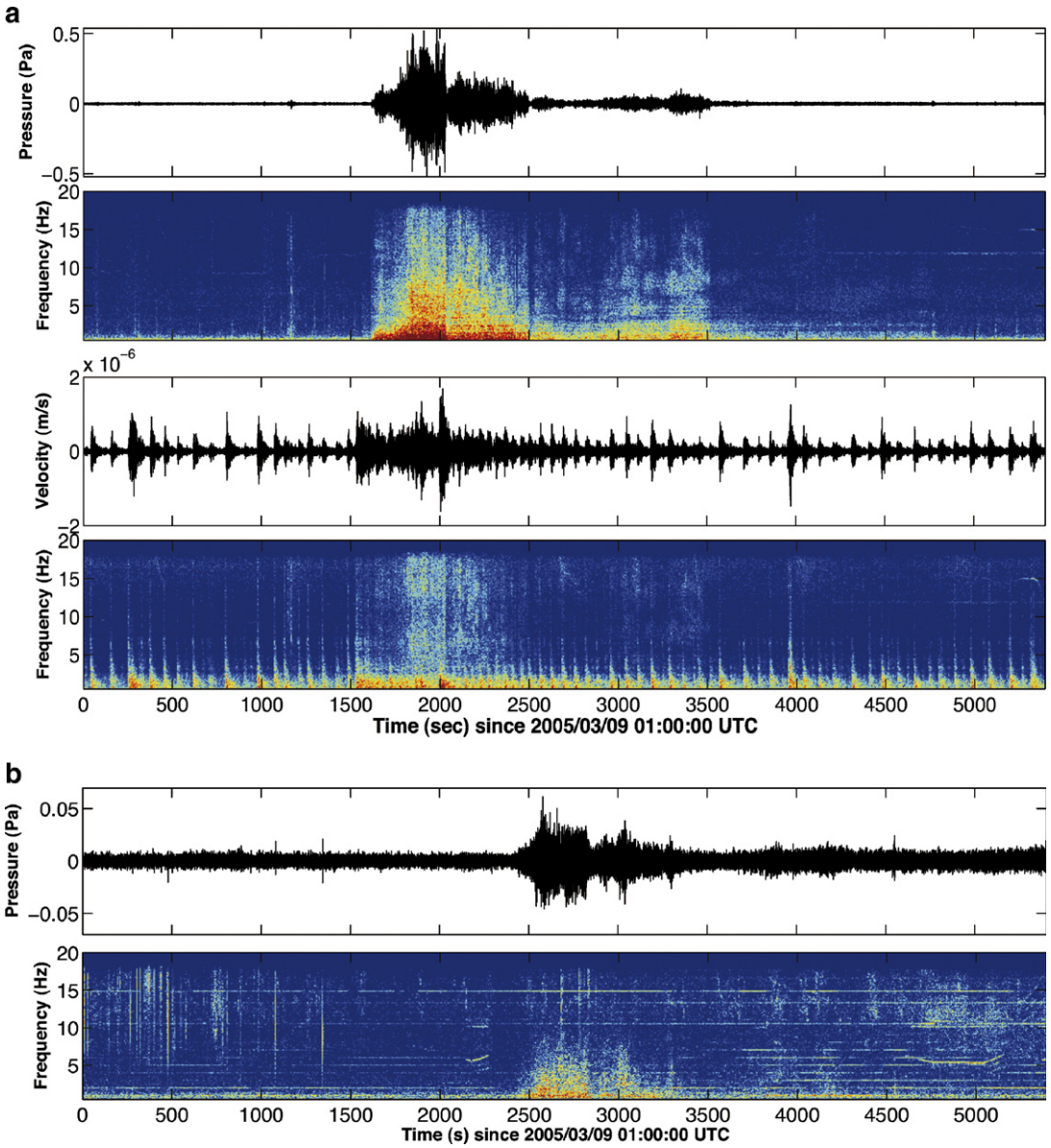

Fig. 8. (a) Waveforms and spectrograms for the March 9th 2005 eruption sequence observed in co-located infrasound (top) and vertical seismic (bottom) sensors at the Coldwater array. The seismic data consist of highly repetitive, discrete LP events occurring before and after the eruption, and merging much closer together during the eruption. In contrast, the infrasound data consist of a quasi-continuous 'roar' of sound observed only during the eruption. An initial ~ 7.2-minute stage with increasing amplitude might result from rapid gas thrusting. This amplitude drops off suddenly and is replaced by a ~ 45.6-minute coda with three distinct sections (see text) which may reflect the subsequent evolution of the gas plume or less vigorous venting from the volcano. Much of this coda contains spectral peaks at ~ 1.5 Hz, ~ 2.5 Hz and other frequencies. (b) The March 9th 2005 eruption signal as observed at the Sacajawea array, ~ 250 km east of Mount St. Helens. The beamformed infrasound data are shown filtered 1–5 Hz. Impulsive signals at the beginning of the record are noise on one channel of the array (see Fig. 9b). The lines of constant frequency present in the spectrogram are continuous harmonic windfarm propellar noise. However, a clear signal originating from the direction of Mount St. Helens begins at ~ 2500 s (~ 01:40 UTC), and lasts ~ 18 min until ~ 3500 s (~ 01:58 UTC).

of PMCC detections at the Coldwater array, spanning ~ 36 h prior to the eruption. Each coherent infrasound detection, regardless of amplitude, is plotted as a dot and color-coded for its frequency content. The main eruption is observed as a small cluster of light blue dots (~ 2–3 Hz) at ~ 11:21:22 UTC. Beginning at ~ 00:00 01/16/05 UTC, a stream of coherent infrasound events are detected for ~ 7 h from the direction of

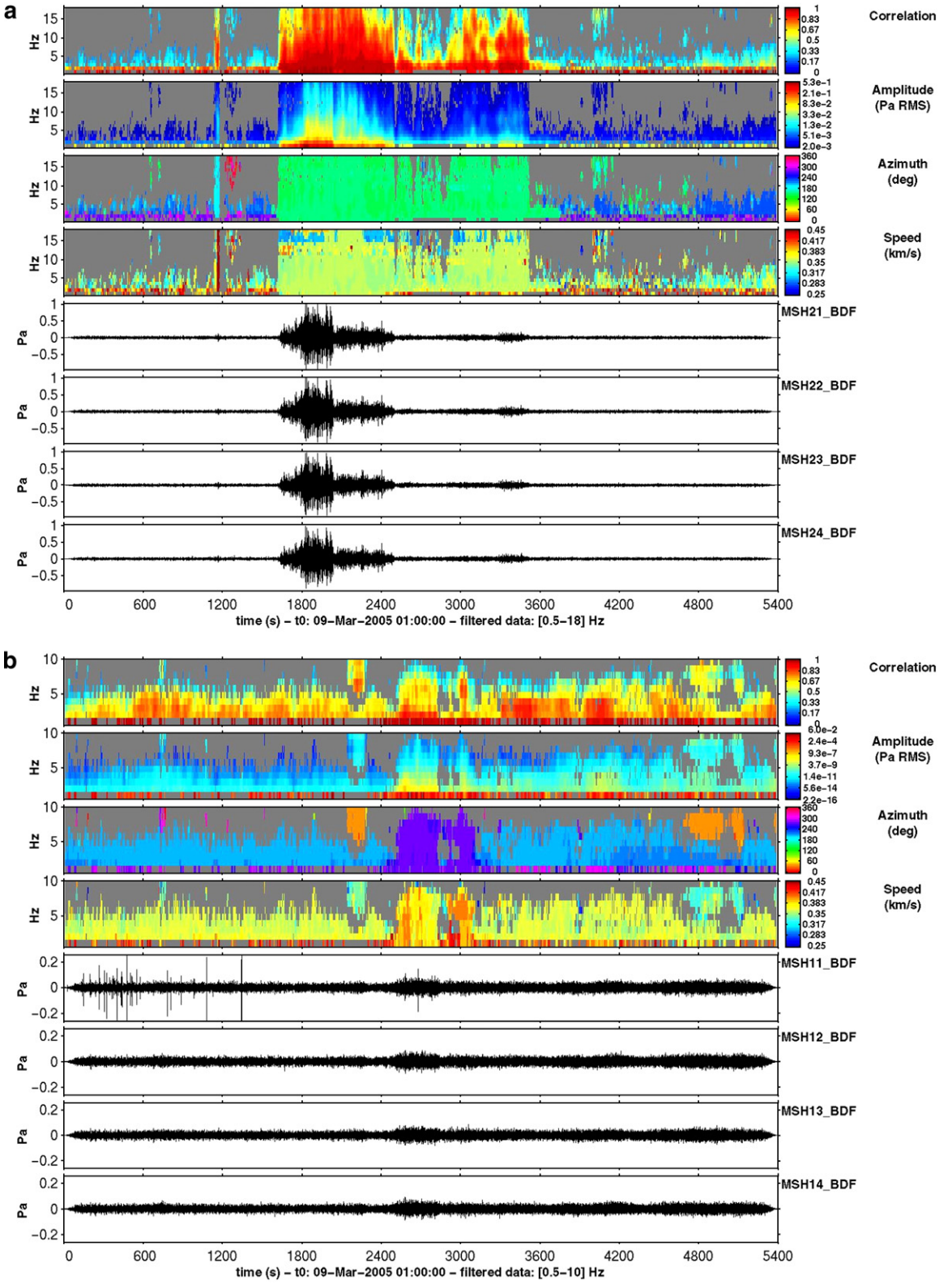
a
Correlation
Amplitude (Pa RMS)
Azimuth (deg)
Speed (km/s)
Hz
Pa
MSH21_BDF
MSH22_BDF
MSH23_BDF
MSH24_BDF
time (s) – t0: 09–Mar–2005 01:00:00 – filtered data: [0.5–18] Hz
b
Correlation
Amplitude (Pa RMS)
Azimuth (deg)
Speed (km/s)
MSH11_BDF
MSH12_BDF
MSH13_BDF
MSH14_BDF
time (s) – t0: 09–Mar–2005 01:00:00 – filtered data: [0.5–10] Hz

Mount St. Helens (~ 160°). The detections are not associated with an increased level of seismicity and are not infrasound twins of LP events. The main burst of activity ends ~ 5 h prior to the eruption. Fig. 7 shows the results of detailed PMCC analysis on 20 min of these signals. The events are of low signal to noise ratio and cannot be distinguished in the raw waveform data. However, PMCC is capable of detecting signals with a low signal to noise ratio. Further work will be required to unravel the significance of these detections.

5.3.2. March 9th 2005 eruption

Fig. 8a shows data recorded at Coldwater during the March 9th 2005 eruption. The top two panels show the beamformed infrasound data and its corresponding spectrogram, while the lower two panels show the co-located vertical seismic channel and its spectrogram. The time series data are shown high pass filtered >1 Hz. Fig. 9a shows the results of detailed PMCC analysis on this time window. The March 9th 2005 eruption signal was initially observed at Coldwater at 01:26:55 UTC, with a coherent signal detectable for ~ 53 min until 02:19:48 UTC. The majority of the energy is below 5 Hz, though the signal is fairly broadband across the infrasound range. The lower amplitude detection at ~ 01:20 UTC is not sourced by Mount St. Helens (wrong azimuth). The waveform is constructed of about four distinct stages. The first stage lasts ~ 430 s between 01:26:55 UTC and 01:34:06 UTC (1615 s to 2045 s on Fig. 8a), and consists of a rapid increase in pressure oscillation amplitude up to a maximum of ~ 0.54 Pa, followed by a sudden drop in pressure amplitude. We interpret this to be the duration of rapid gas thrusting, during which the volcano was ejecting steam and ash at high velocity. At 2045 s, a second broadband packet of energy is present, abruptly terminating at 2515 s. This is followed by a third, lower amplitude stage (2515 s to 3520 s) with spectral structure evolving between ~ 2900 s and 3520 s to include higher frequencies. Finally, after 3520 s, a low amplitude coda rings on for ~ 20 min, which is clearly identified in the PMCC analysis (Fig. 9a).

There is some spectral structure evident in the latter three stages. Well-defined spectral peaks at ~ 1.5 Hz, and ~ 2.5 Hz are present in every stage after the initial ~ 430 s 'gas thrusting' stage along with other transiently appearing spectral peaks. The peaks at ~ 1.5 Hz and ~ 2.5 Hz are most visible in the final ~ 20-minute stage (Fig. 8a). These subsequent stages may correspond to either the evolution of the gas plume as it continued to generate infrasound by turbulent convection, or a lower amplitude jetting noise associated with slower, steadier venting.

Fig. 8b shows the beamformed infrasound at Sacajawea. The time series is shown bandpass filtered between 1 and 5 Hz. Impulsive signals at the beginning of the record are noise local to channel 1 of the array (Fig. 9b). The lines of discrete constant frequency present in the spectrogram are a record of continuous windfarm propeller noise. However, a clear signal originating from the direction of Mount St. Helens begins at ~ 01:40 UTC, and lasts ~ 18 min until ~ 01:58 UTC. The signal is easily distinguished from the background noise by the arrival azimuth derived from PMCC and its spectral signature (Fig. 9b). The signal has essentially the same frequency-domain characteristics as that recorded at the Coldwater array, though much of the energy above 10 Hz has been attenuated. In the time domain, approximately the same waveform structure is apparent, though the amplitude has diminished to ~ 0.05 Pa, and the detectable signal is shorter. The signal arrives at Sacajawea ~ 13 min later than at Coldwater, which is consistent with the 250 km geographic distance between the array sites. A more detailed look at these arrival times and relative amplitudes using propagation through atmospheric velocity models is necessary to discern the exact propagation path and attenuation characteristics of the pressure wave. This is beyond the scope of this paper and will be addressed in a future publication.

6. Discussion

6.1. Infrasonic long period events

The observation that the source that generates LP events also generates infrasound is of high significance. In November 2005, an observer standing in the summit region reported feeling seismic LP events, and hearing

Fig. 9. (a) Detailed PMCC analysis of the March 9th, 2005 eruption signal. Time range is identical to that shown in Fig. 8. The top four panels show the frequency content of the signal vs. time, color-shaded according to the parameter labeled on the right-hand side. Correlation is that between different sensors of the array. Amplitude, azimuth, and speed describe how the signal propagated across the array. The lowermost four panels show the sensor time series data. A coherent signal associated with the eruption, and coming from the direction of Mount St. Helens (lime green in the azimuth panel) is detected for ~ 52.8 min from 01:26:55 UTC until 02:19:48 UTC. The lower amplitude detection preceding the eruption at ~ 01:20 UTC is not sourced by Mount St. Helens (wrong azimuth). (b) Detailed PMCC analysis of the March 9th, 2005 eruption signal observed at the Sacajawea array, ~ 250 km from Mount St. Helens. A coherent signal associated with the eruption, and coming from the direction of Mount St. Helens (purple in the azimuth panel) is detected for ~ 18 min from ~ 01:40 UTC until ~ 01:58 UTC.

associated acoustic 'booms' (Seth Moran, CVO/USGS, personal communication). This suggests that close to the volcano, at least some of the energy is also in the audible acoustic range (>20 Hz). LP events are often modeled by an initial pressure excitation mechanism, followed by a coda resulting from resonance in a fluid-filled conduit or crack (Chouet, 1985, 1988, 1992, 1996; Garcés, 1997; Neuberg et al., 2000). LP events may also be considered the impulse response of the resonant tremor-generating system (Chouet, 1985), although the excitation mechanisms involved in both cases remain incompletely understood (Chouet, 1996). The absence of a prominent infrasound coda (Fig. 4b) may indicate that the infrasound is more representative of the excitation mechanism of LP events. Also, one must explain the observation that not all seismic LP events have associated infrasonic twins (Fig. 3, or compare Figs. 4 and 5).

Infrasound twins of LP events could be sourced in three ways: 1) direct seismo-acoustic coupling at the ground–air interface by a ground-piston effect; 2) a pressure excitation function in a fluid that produces acoustic oscillations in the fluid (leading to seismic LP events), and a pressure wave in the air (leading to infrasound twins) or 3) a pressure disturbance accompanied by a rapid release of gas, which travels to the surface through a permeable medium and generates infrasound twins.

In case (1), the cessation and reemergence of infrasound twins could be attributed to factors influencing the propagation of the seismic wave to the surface. Examples of factors include changes in the source depth, or magnitude, or changes in the impedance contrast at the ground–air interface.

In cases (2) and (3), the switching on and off of LP infrasound may reflect changes in the vesicularity and permeability of the system, or contain information about the fragmentation dynamics (Garces et al., 2004). Observation of infrasound twins would indicate that the pathways for infrasound or gas transmission are more open, while absence of infrasound twins would indicate that the pathways are sealed. Further work will need to focus on the role of earthquake magnitude and location (particularly depth) in influencing seismic to acoustic coupling, and a more detailed comparison of the seismic LP events and their infrasonic counterparts in the time and frequency domains is required.

Alternatively, variations in the detection of infrasonic LP events may be controlled by variations in atmospheric conditions between the volcano and the Coldwater array, or a change in the background noise level at the array. However, in many cases infrasonic LP events emerge and disappear without correlation with wind speed or direction, temperature, or a change in the background noise level at the array, and without change in detections from other sources (Fig. 3). This suggests that this is a source effect, and not a propagation or a detection (signal:noise ratio) effect. Moderate winds induce azimuthal scatter in *all* detections at the array simultaneously, while very strong winds result in the loss of all coherent signal. This said, the wind sensor is co-located with the array in the dense forest, and is somewhat protected from regional winds. Therefore, data on the atmospheric conditions along the propagation path between the volcano and the Coldwater array are needed to fully rule out propagation effects. This question could be addressed with the addition of an exposed wind sensor between the volcano and the Coldwater array, and perhaps the addition of infrasonic sensors placed closer to the volcano. An array of sensors would enable distinction between acoustic energy and vibration of sensors by seismic ground motion (Moran et al., in press) since the seismic — acoustic time-delay would be shorter closer to the source.

6.2. Eruption infrasound

The observation of clear infrasonic signals associated with the January 16th and March 9th 2005 eruptions is encouraging from both a scientific and monitoring perspective. Infrasound places tight constraints on the exact timing of eruptive activity because a drastic surge in infrasonic energy coincides with the eruption period. The January 16th eruption further demonstrates the utility of infrasound observations for monitoring, as the eruption was essentially aseismic, and visually obscured by cloud cover. In contrast, the acoustic record reveals a 7-hour duration of heightened infrasound activity prior to the eruption, and a clear record of the eruption itself. Equally, the observation of the March 9th eruption at Sacajawea (~ 250 km away) indicates that infrasound can be used as a long range monitoring tool for modest-sized eruptions, even with relatively small aperture arrays.

Infrasound also provides a means to quantitatively compare the power of eruptions (Johnson et al., 2003). At Coldwater, the January 16th eruption signal reached a maximum amplitude of ~ 0.065 Pa. Assuming a spherical spreading factor of $1/R$ for the 13.41 km distance from volcano to array, the sound pressure level ~ 1 m from the source would have been ~ 872 Pa, or ~ 153 dB re 20 μPa. If this sound were in the audible frequency range, it would be as loud as a jet engine during takeoff. The amplitude of the March 9th eruption signal reached 0.54 Pa, an order of magnitude larger

than that of the January 16th eruption. In this case, using $1/R$ to correct for spherical spreading, the sound pressure level ~ 1 m from the source would have been ~ 6571 Pa, or ~ 171 dB re 20 μPa.

Figs. 5 and 8a also reveal that acoustic signatures of eruptions are notably different from their seismic signatures. For the March 9th eruption (Fig. 8a), the acoustic signature was a four-stage, quasi-continuous signal with evolving spectral structure. In contrast, the seismicity consisted of an intense swarm of individual LP events, merging closer together in time during the eruption. The acoustic data may therefore represent the shallower processes of pressure release, gas and ash venting, and perhaps subsequent evolution of the volcanic plume, and not the deeper processes that act as seismic sources. In this respect, joint seismic and acoustic studies are capable of reconstructing the entire wavefield generated by the volcano. Waveform modeling of joint infrasound and seismic observations can therefore lead to an enhanced understanding of the physics of the eruption process.

7. Conclusions

Infrasound observations complement seismic observations, allowing one to record the complete wavefield radiated by volcanoes. Mount St. Helens almost continuously generated infrasound during the November 2004–March 2005 deployment. Infrasound twins of long period (LP) events are closely related to their seismic counterparts and must be sourced simultaneously, though not necessarily by simple seismo–acoustic coupling. Future models of the source mechanism for LP events should therefore explain the radiated infrasound. In contrast, infrasound observed during eruptions is distinctly different from simultaneous seismic observations. The active gas and ash venting stage of the eruption generates a very large, unambiguous surge in infrasonic energy, which can be detected at long range (at least 250 km). In contrast, the seismicity observed during the eruption is of about the same amplitude as the preceding seismicity. Infrasound can therefore play a key role in separating surface processes from deeper processes, and in identifying the timing and vigor of eruptions. The infrasound array deployment at Mount St. Helens will continue, and analysis of the resulting data set will be further developed in future work.

Acknowledgements

This experiment would not have been possible without the support of the Geological Survey of Canada (the GSC). Contributions by members of the GSC team were manifold. The team is led by David McCormack (Head, Earthquake Tsunami and Volcano Hazard Assessment and the Nuclear Monitoring Program). Phil Munro helped in locating the arrays and obtaining permission to use the land. Calvin Andrews, John Ristau, Issam Al-Khoubbi, Jim Helferty, Kadircan Aktas, and Mike Patton helped deploy the arrays. Tim Côté, and Luc Saumure provided much assistance with data acquisition and archiving. The GSC provided most of the equipment for this experiment. This experiment was conducted as part of the Acoustic Surveillance for Hazardous Eruptions (ASHE) program, a pilot study on the feasibility of providing advance warnings to the aviation industry. This program is led by David McCormack, Hank Bass (director of the National Center for Physical Acoustics at the University of Mississippi) and Milton Garcés. Clint Coon and Eric Blum (UCSD) helped deploy the arrays. David Norris (BBN) performed ray tracing to determine the Sacajawea location. Lengthy discussions with the team at ISLA/UHM (David Fee, Sara McNamara, Claus Hetzer), Seth Moran (CVO/USGS), Kris Walker (UCSD), and David Green (Univ. Leeds) greatly helped shape ideas. Fig. 1 was made using GMT, with a DEM provided by USGS seamless, and help from David Sherrod, Steve Schilling, Wes Thelen and Seth Moran. We would like to thank Alexis Le Pichon and an anonymous reviewer for careful and constructive comments that helped to improve the clarity of this manuscript. This work was funded in part by the National Science Foundation (grant EAR-0609669).

References

Arrowsmith, S.J., Hedlin, M.A.H., 2005. Observations of infrasound from surf in southern California. Geophysical Research Letters 32, L09810. doi:10.1029/2005GL022761.

Bedard, A.J., Georges, T.M., 2000. Atmospheric infrasound. Physics Today 53 (3), 32–37.

Brown, D., Tupper, T., Christie, D., Itikarai, I., 2005. Multi-technology observations of the Manam volcano eruption in January 2005 — potential for an enhanced volcanic ash warning system. 2005 Infrasound Technology Workshop, Tahiti.

Cansi, Y., 1995. An automatic seismic event processing for detection and location: the P.M.C.C. method. Geophysical Research Letters 22 (9), 1021–1024.

Cansi, Y., Klinger, Y., 1997. An automated data processing method for mini-arrays. Newsletter of the European–Mediterranean Seismological Centre 11, 2–4.

Chouet, B., 1985. Excitation of a buried magmatic pipe: a seismic source model for volcanic tremor. Journal of Geophysical Research 90, 1881–1893.

Chouet, B., 1988. Resonance of a fluid-driven crack: radiation properties and implications for the source of long-period events

and harmonic tremor. Journal of Geophysical Research 93, 4375–4400.
Chouet, B., 1992. A Seismic Model for the Source of Long-Period Events and Harmonic Tremor. In: Gasparini, P., Scarpa, R. (Eds.), IAVCEI Proceedings in Volcanology, vol. 3, pp. 133–156.
Chouet, B.A., 1996. Long-period volcano seismicity: its source and use in eruption forecasting. Nature 380, 309–316.
DeFatta, D.J., Lucas, J.G., Hodgkiss, W.S., 1988. Digital Signal Processing: A System Design Approach. John Wiley, NY.
Dzurisin, D., Vallance, J.W., Gerlach, T.M., Moran, S.C., Malone, S.D., 2005. Mount St. Helens reawakens. EOS 86 (3), 25–29.
Fee, D., McNamara, S., Garces, M., Bortz, W., Hoblitt, R., Trusdell, F., 2005. Diurnal variations in infrasonic Tremor signals from Kilauea volcano, Hawaii. 2005 Infrasound Technology Workshop, Tahiti.
Garcés, M., 1997. On the volcanic waveguide. Journal of Geophysical Research 102 (B10), 22,547–22,564.
Garcés, M., Hansen, R.A., 1998. Waveform analysis of seismoacoustic signals radiated during the Fall 1996 eruption of Pavlof volcano, Alaska. Geophysical Research Letters 25 (7), 1051–1054.
Garcés, M.A., Hagerty, M.T., Schwartz, S.Y., 1998. Magma acoustics and time-varying melt properties at Arenal Volcano, Costa Rica. Geophysical Research Letters 25 (13), 2293–2296.
Garcés, M., Iguchi, M., Ishihara, K., Morrissey, M., Sudo, Y., Tsutsui, T., 1999. Infrasonic precursors to a Vulcanian eruption at Sakurajima Volcano, Japan. Geophysical Research Letters 26 (16), 2537–2540.
Garcés, M., Harris, A., Hetzer, C., Johnson, J., Rowland, S., Marchetti, E., Okubo, P., 2003. Infrasonic tremor observed at Kilauea Volcano, Hawai'i. Geophysical Research Letters 30 (20). doi:10.1029/2003GL018038.
Garces, M., Marchetti, E., Ripepe, M., 2004. Acoustic oscillations in volcanoes. Eos, Transactions of the American Geophysical Union 85 (47) (Fall Meet. Suppl., Abstract V13D-01).
Garcés, M., Aucan, J., Fee, D., Caron, P., Merrifield, M., Gibson, R., Bhattacharyya, J., Shah, S., 2006. Infrasound from large surf. Geophysical Research Letters 33, L05611. doi:10.1029/2005GL025085.
Green, D.N., Neuberg, J., 2005. Seismic and infrasonic signals associated with an unusual collapse event at the Soufrière Hills volcano, Montserrat. Geophysical Research Letters 32, L07308. doi:10.1029/2004GL022265.
Guilbert, J., Harjadi, P., Purbawinata, M., Jammes, S., Le Pichon, A., Feignier, B., 2005. Monitoring of Indonesian volcanoes with infrasound: preliminary results. 2005 Infrasound Technology Workshop, Tahiti.
Hagerty, M.T., Schwartz, S.Y., Garcés, M.A., Protti, M., 2000. Analysis of seismic and acoustic observations at Arenal Volcano, Costa Rica, 1995–1997. Journal of Volcanology and Geothermal Research 101, 27–65.
Hedlin, M.A.H., Garces, M., Bass, H., Hayward, C., Herrin, G., Olson, J., Wilson, C., 2002. Listening to the secret sounds of Earth's atmosphere. EOS 83, 564–565 (557 pp.).
Hedlin, M.A.H., Alcoverro, B., D'Spain, G., 2003. Evaluation of rosette infrasonic noise-reducing spatial filters. Journal of the Acoustical Society of America 114 (4), 1807–1820.
Johnson, J.B., Aster, R.C., 2005. Relative partitioning of acoustic and seismic energy during Strombolian eruptions. Journal of Volcanology and Geothermal Research 148, 334–354.
Johnson, J.B., Aster, R.C., Ruiz, M.C., Malone, S.D., McChesney, P.J., Lees, J.M., Kyle, P.R., 2003. Interpretation and utility of infrasonic records from erupting volcanoes. Journal of Volcanology and Geothermal Research 121, 15–63.
Johnson, J.B., Aster, R.C., Kyle, P.R., 2004. Volcanic eruptions observed with infrasound. Geophysical Research Letters 31, L14604. doi:10.1029/2004GL020020.
Johnson, J.B., Lees, J.M., Yepes, H., 2006. Volcanic eruptions, lightning, and a waterfall: differentiating the menagerie of infrasound in the Ecuadorian jungle. Geophysical Research Letters 33, L06308. doi:10.1029/2005GL025515.
Lahr, J.C., Chouet, B.A., Stephens, C.D., Power, J.A., Page, R.A., 1994. Earthquake classification, location, and error analysis in a volcanic environment: implications for the magmatic system of the 1989–1990 eruptions of Redoubt Volcano, Alaska. Journal of Volcanological and Geothermal Research 63, 137–151.
Moran, S.C., 2005. Overview of seismicity associated with the 2004–2005 Eruption of Mount St. Helens. AGU meeting. Fall 2005, session V52B.
Moran, S.C., McChesney, P.J., Lockhart, A.B., in press. Seismicity and infrasound associated with explosions at Mount St. Helens, 2004–2005, chap. 6. In: Sherrod, D.R., Scott, W.E., Stauffer, P.H., (Eds.), A Volcano Rekindled: The First Year of Renewed Eruptions at Mount St. Helens, 2004–2006. U.S. Geological Survey Professional Paper.
Neuberg, J., Luckett, R., Baptie, B., Olsen, K., 2000. Models of tremor and low-frequency earthquake swarms on Montserrat. Journal of Volcanology and Geothermal Research 101, 83–104.
Rambolamanana, G., Ramanantsoa, A., Andriamiranto, R., 2005. Madagascar infrasound station I33S and the observed signals. 2005 Infrasound Technology Workshop, Tahiti.
Reed, J.W., 1987. Air pressure waves from Mount St. Helens eruptions. Journal of Geophysical Research 92, 11979–11992.
Ripepe, M., Marchetti, E., 2002. Array tracking of infrasonic sources at Stromboli volcano. Geophysical Research Letters 29 (22), 33-1–33-4. doi:10.1029/2002GL015452.
Strachey, R., 1888. On the Air Waves and Sounds Caused by the Eruption of Krakatoa in August, 1883. In: Simkin, T., Fiske, R.S. (Eds.), Krakatau 1883 (published 1983). Smithsonian Institution Press, pp. 368–374.
Yamasato, H., 1997. Quantitative analysis of pyroclastic flows using infrasonic and seismic data at Unzen Volcano, Japan. Journal of Physics of the Earth 45 (6), 397–416.